Air side thermal performance of wavy fin heat exchangers produced by selective laser melting

J Kuehndel[1,2], B Kerler[1], C Karcher[2]
[1] Mahle Industrial Thermal Systems, Heilbronner Straße 380, 70469 Stuttgart, Germany
[2] Institute of Thermodynamics and Fluid Mechanics, Technische Universität Ilmenau, PO Box 100565, 98684 Ilmenau, Germany

E-mail: jonas.kuehndel@mahle.com

Abstract. Wavy fins are widely used for off-road vehicle coolers, due to their dust resistance. In this study, heat exchanger elements with wavy fins were examined in an experimental study. Due to independence of tooling and degrees of freedom in design, rapid prototyping technique selective laser melting was used to produce heat exchanger elements with high dimensional accuracy. Tests were conducted for air side Reynolds number Re of 1400 –7400 varying wavy amplitude and wave length at a constant water flow rate of 9.0m³/h inside the tubes. The effects of wavy amplitude and wave length on the air side thermal performance were studied. Experimental correlation equations for Nu and ψ were derived by regression analysis.

1. Introduction

Thermal management has become more important in recent years due to its potential to save energy, especially in vehicle applications. As crucial element of thermal management heat exchanger, i.e. radiators, charge air coolers, evaporators and condensers are designed to ensure the engine's function and to provide air conditioning. Due to the dominant thermal resistance on the air side of heat exchangers, an improvement of heat exchangers can be realized by enhancing the air side convection heat transfer coefficient, derived by fin optimization. Different fin geometries e.g. plain fins, louvered fins, offset strip fins and wavy fins are used in compact heat exchangers. However, the latter are beneficial with respect to their resistance to dust adherence and their thermal hydraulic performance.

In wavy fins and at laminar flow regime, the swirl flow induced by wall corrugations gives the fluid a movement perpendicular to the main flow direction, thus mixing the flow and increasing the heat transfer [1][2]. Dong et al. [1][3][4] developed experimental correlations depicting thermal hydraulic performance of wavy fins. They investigated the effect of geometry parameters on thermal hydraulic performance of wavy fins in studies and showed that wavy length and wavy fin amplitude have the superior impact on the thermal hydraulic performance. Thus, the present study focusses on these two geometric parameters.

A limiting factor of the experimental studies with wavy fins is the dependence on tooling, as wavy fins are generally produced by rolling or stamping to produce a high number of respective fin geometry at low costs. Moreover, Joshi et. al. [5] reports on manufacturing irregularities i.e. edge roundness and burred edges have impact on thermal hydraulic measurements. For these reasons and to avoid high tooling costs and to take benefit from the high degree of freedom in creating desired geometries, the process of selective laser melting (SLM) was used to produce the heat sinks [6]. Wong

et al. [7] revealed the potential of SLM for heat sink production. They performed thermal hydraulic measurements with 4 different heat sink geometries produced by SLM due to their geometric complexity and showed their superior performance compared to conventional heat sinks. A side effect of SLM is a higher surface roughness. Strano et al. [8] conducted experiments measuring the surface roughness of a structure produced by SLM. The result was a model depicting surface roughness dependent on the build orientation in the SLM-process. Ventola et al. [9] also performed experiments stating the potential of SLM for usage in electronics cooling. Benefitting from the rough surfaces due to SLM, they found heat transfer can be enhanced by 35% compared to a smooth single finned surface.

In the present paper, a new method of fin development using SLM and experimental test bench results is introduced. This paper is organized as follows. In section 2 we depict test bench, heat sink geometries, test conditions and evaluation method. In section 3 results are presented and discussed. Finally, in section 4 main conclusions and outlook are provided.

2. Methodology

2.1 Test bench

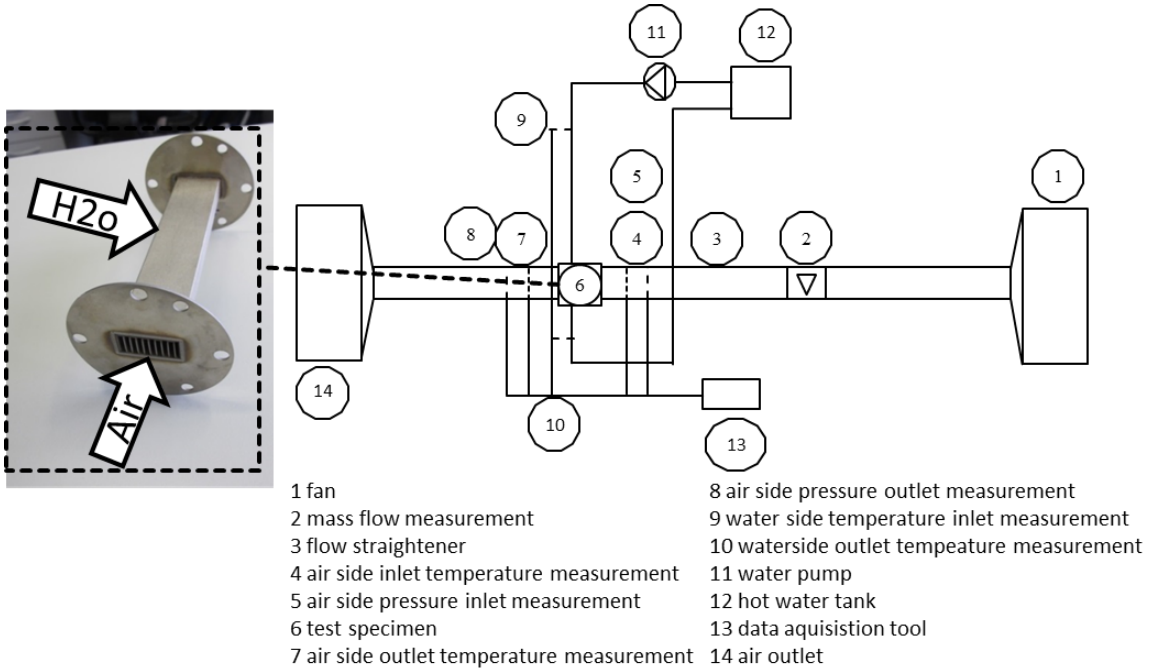

Figure 1. Test specimen with flow arrangement and simplified illustration of the test bench.

Figure 1 depicts the test apparatus for the thermal hydraulic measurements in this study schematically. The test bench consists of a closed water side circuit, an open air side circuit, test specimen and measurement tools. The two mass flows are led together in a cross-flow as shown in figure 1, heating the air inside in the test specimen. The water side circuit with the hot water tank and the pump circulates water around the test specimen. Inlet and outlet temperature of the water side are measured by two pre-calibrated Pt100 resistance thermometers within an accuracy of 0.1K very close to the inlet and outlet. Moreover, the water channel was isolated. V-cone flow meter for mass flow determination and precision differential pressure transducers for pressure drop measurement were installed. The open air side circuit provides mass flow on the air side with a fan to charge the different fin geometries with various mass flow rates. Similar to the water side, inlet and outlet temperature measurements on the air

side are detected by two pre-calibrated Pt100 resistance thermometers within an accuracy of 0.1K. V-cone flow meter and precision differential pressure transducers measured mass flow and pressure drop, respectively

2.2 Heat sink geometries

Figure 2 shows the varying geometry parameters of a wavy fin. The heat exchanger elements were produced by SLM with a M1 Concept laser machine using stainless steel 316L. Table 1 gives the technical details of the test specimen. Nine different heat exchanger elements were tested with an air flow length of L=150mm, a fin height of F_h=12mm, test element width of F_w=30mm and a fin thickness of t=0.3mm. The dimensional accuracy of the test specimen tested by metallographic analysis is within an accuracy of ±0.1mm. Moreover, porosity was defined with metallographic examination of the test elements as <1% as seen in figure 3 and therefore the impact of porosity on the thermal hydraulic measurements can be neglected.

Table 1. Geometric specification of the test elements

No	Wavy length WL (mm)	Wavy amplitude $2A$ (mm)	$2A/WL$ (-)
1	12.5	2	0.16
2	7.5	1	0.13
3	7.5	1.5	0.20
4	12.5	1	0.08
5	7.5	2	0.27
6	10	1	0.10
7	10	1.5	0.15
8	12.5	1.5	0.12
9	10	2	0.20

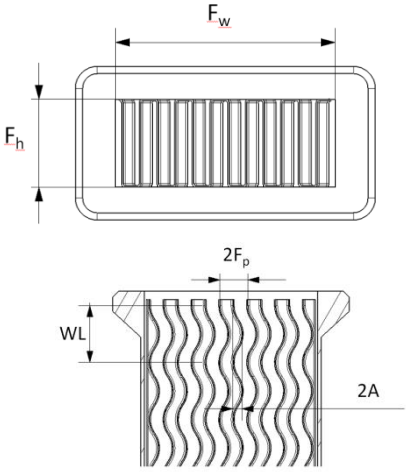

Figure 2. Geometric parameters of wavy fin and test specimen.

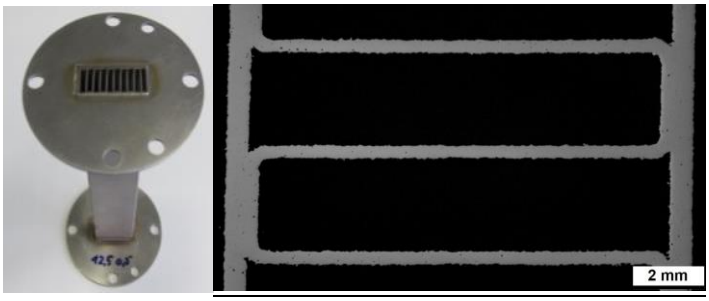

Figure 3. Test specimen and metallographic examination of test specimen with density >99%.

2.3 Test conditions

Air mass flow rate m_{air} was varied from 0.002 to 0.01kg/s, resulting a Re range from 1400-7400, as defined by equation (1):

$$Re = \frac{u d_h}{\nu} \quad (1)$$

Here, u denotes the average flow velocity, ν represents the kinematic viscosity. The assumptions of air as an incompressible fluid was made and substance data of air was considered constant to logarithmic air temperature. The hydraulic diameter d_h can be defined as:

$$d_h = \frac{4 * A_{free} * V}{A_0 * A_{front}} \quad (2)$$

The heat exchanger volume V, frontal area A_{front}, the total air side heat surface area A_0 and the air side minimum free flow area A_{free} are needed for this definition. On the water side, the inlet temperature is 90°C with a constant water flow rate of 9.0m³/, engendering a water side *Re* = 40000 and Nusselt Numbers *Nu* = 152 as defined by:

$$Nu = \frac{\alpha * d_h}{\lambda} \quad (3)$$

λ is the thermal conductivity and α the heat transfer coefficient. The difference of the water side inlet and out temperature $t_{h2o,in} - t_{h2o,out}$ was smaller than 0,5K. Thus, a dominance of the water side heat transfer is guaranteed and an isothermal wall temperature at the specimen can be assumed. The data was accessed under stationary conditions.

2.4 Evaluation method

The heat transfer rate for the air side Q_{air} can be obtained by

$$Q_{air} = m_{air} * c_{p,air} * (t_2 - t_1) \quad (4)$$

Here, $c_{p,air}$ is specific heat at constant pressure for air, t_2 and t_1 represent the outlet and inlet air temperature, respectively. By assuming the heat transfer rate for the air side Q_{air} being equal to the heat transfer rate for the water side, we define heat transfer effectiveness Φ for every measurement point as

$$\Phi = \frac{Q_{air}}{m_{air} * c_{p,air} * (t_1 - t_{h2o})} \quad (5)$$

with the temperature of the water t_{h2o}. The overall heat transfer coefficient kA for the test specimen is:

$$kA = m_{air} * c_{p,air} * NTU \quad (6)$$

Here, NTU is the number of transfer units. Heat transfer coefficient air side α_{air} is calculated with equation (7). Note that the term representing the water side heat resistance can be neglected due to the dominance of the water side heat transfer resulting in a very high heat transfer coefficient α_{h20}.

$$\frac{1}{\alpha_{air} * \eta_a * A_0} = \frac{1}{kA} - \frac{s_t}{\lambda_t A_t} - \frac{1}{\alpha_{h20} A_{h2o}} \quad (7)$$

s_t, λ_t and A_t are thickness, heat conductivity and heat surface area of the tube, respectively. Surface effectiveness η_a and fin efficiency η_f of the wavy fins are defined as:

$$\eta_a = 1 - \frac{\mathrm{A_f}}{A_0}(1 - \eta_f) \tag{8}$$

$$\eta_f = \frac{tanh(m * l)}{m} \quad m = \left(\frac{2\alpha_{air}}{\lambda_f * t}\right)^{0,5} \quad l = 0{,}5F_h \tag{9}$$

λ_f and $\mathrm{A_f}$ are the thermal heat conductivity and the surface area of the fin, respectively. With an iterative calculation, α_{air} can be gained from equations (7)-(9). Finally, air side Nusselt number Nu can be calculated with equation (3). In order to evaluate pressure drop we calculate Darcy friction factor ψ which can be defined as:

$$\psi = \frac{d_h * \Delta p}{0.5L * \rho * u^2} \tag{10}$$

Here, Δp and ρ denote the pressure drop and density, respectively. In order to evaluate the measurement results, a goodness factor *JF* is introduced:

$$JF = \frac{Nu}{\psi} \tag{11}$$

As defined in equation (12), $\delta_l(x)$ represents the thickness of the laminar boundary layer on a horizontal flow board in dependence of the the flow length x, u and ν. $\delta_t(x)$ denotes the thickness of the viscous sublayer in turbulent regime on a horizontal flow board [10]. An evaluation of $\delta_l(x)$ and $\delta_t(x)$ becomes necessary for identifying the impact of surface roughness on the measurements.

$$\delta_l(x) = 5\left(\frac{x * \nu}{u}\right)^{0.5} \tag{12}$$

$$\delta_t(x) = \frac{50x}{Re_x\left(0.5c_f\right)^{0.5}} \tag{13}$$

With Adams et al. [11] a equivalent sand grain roughness k_s can be calculated as function of average surface roughness $\mathrm{R_a}$ as defined by:

$$k_s = 5.863 * R_a \tag{13}$$

Taking into account instrument errors, geometry tolerances and property uncertainties, the estimated uncertainties for the Nu and ψ are 7.9% and 5.4%, respectively.

3. Results

Results are presented as Nusselt numbers Nu and Darcy friction factors ψ against Re to express the influence of wavy length *WL* and wavy amplitude *2A* on heat transfer and pressure drop performance with measurement points and correlations. Figure 4 shows the effect of WL on Nu and ψ at constant WL=12.5mm and a varying *2A*. As expected, an increasing wavy amplitude *2A* leads to a higher Nu and ψ with a double wavy amplitude causing an increase in Nu and ψ up to 34% and 39%, respectively. Figure 5 depicts Nu and ψ as function of Re for a constant $2A$=2mm and a varying WL. It can be seen that a reduction of WL from 12.5mm to 7.5mm leads to an increase in Nu and ψ up to 45% and 77%, respectively. To conclude, a lower wavy amplitude to wavy length ratio $2A/WL$ shows

an increasing effect on Nu and ψ. This can be explained by an enhanced mixing of the flow and vortex generation, thus creating higher pressure drop and heat transfer, as also found by [1][2][3].

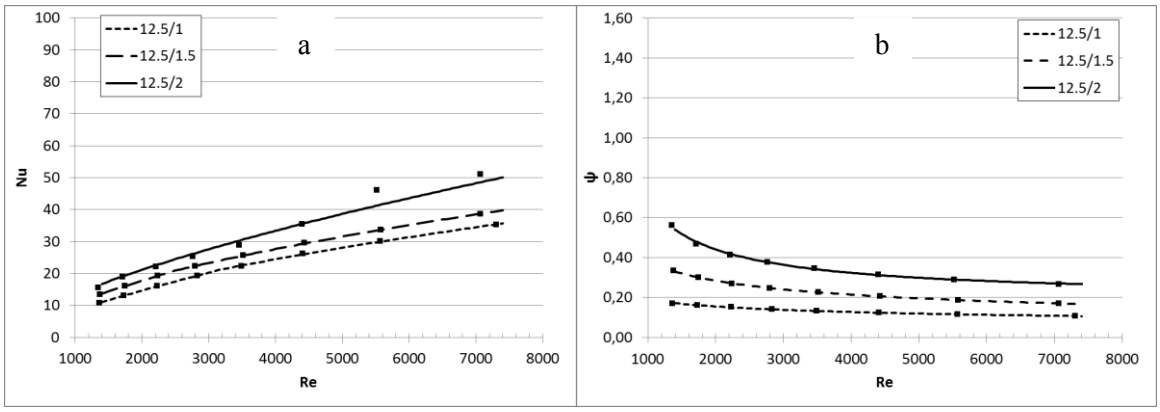

Figure 4. Nusselt number *Nu* (a) and Darcy friction factor ψ (b) as function of Reynolds number *Re* for a constant wavy length *WL* of 12.5mm and varying wavy amplitude *2A* from 1mm to 2mm.

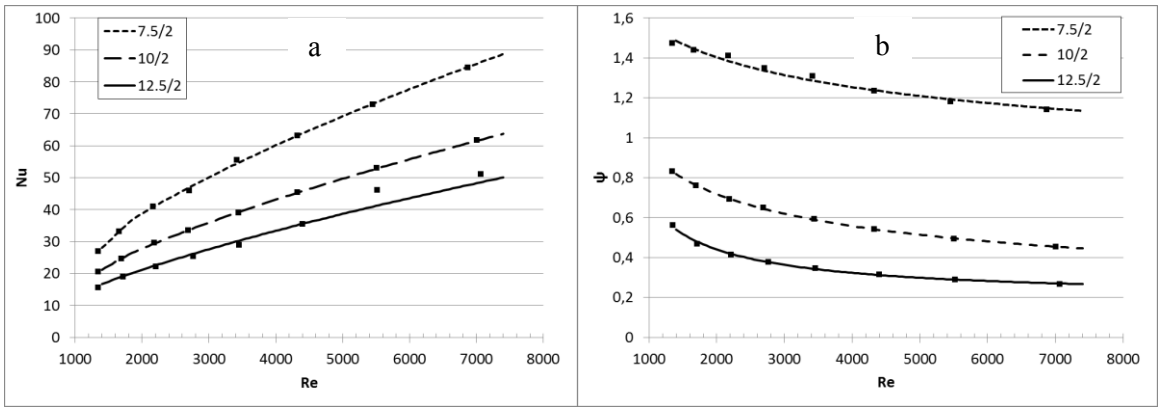

Figure 5. Nusselt number *Nu* (a) and Darcy friction factor ψ (b) as function of Reynolds number *Re* for a constant wavy amplitude *2A* of 2mm and varying wavy length *WL* from 7.5mm to 12.5mm.

As $2A/WL$ has been identified as the superior influence factor on thermal hydraulic performance [1], the goodness factor of the measurement results with various $2A/WL$ against Re is shown in figure 6. A trend is revealed that JF is better for small $2A/WL$. If the test specimen with the same $2A/WL$=0.2 are compared, it is indicated that increasing $2A$ and WL for a constant $2A/WL$ have a better JF. That is also verified by the experimental correlation of Dong et al. [1].

As mentioned above, SLM causes higher surface roughnesses. Strano et al. [9] conducted a study of the effect of build orientation in the process of SLM on the surface roughness. As a result, the maximum of surface roughness is found at R_a=17.0µm for a structure consisting of stainless steel 316L, which is the same material used for building the heat sink geometries. Using equation (13), an equivalent sand grain roughness k_s=99.7µm can be calculated. Comparing equivalent sand grain roughness k_s=99.7µm to $\delta_l(x)$, it can be shown with equation (12) that after a flow length of 0.07mm at Re=2210, laminar boundary layer has reached the same heigth as maximum k_s at maximum Re in laminar regime. For maximum Re=7400 in turbulent regime the thickness of the viscous sublayer $\delta_t(x)$ at a flow length of 1.1mm has reached the same height as maximum k_s. This indicates that

surface roughness to have no effect on the measurements as beyond that point δ is higher than k_s and 1.1mm compared to the total flow length L of 150mm is neglectiable small. The impact of surface roughness will be examined by further experiments as well as by computational fluid dynamics simulations.

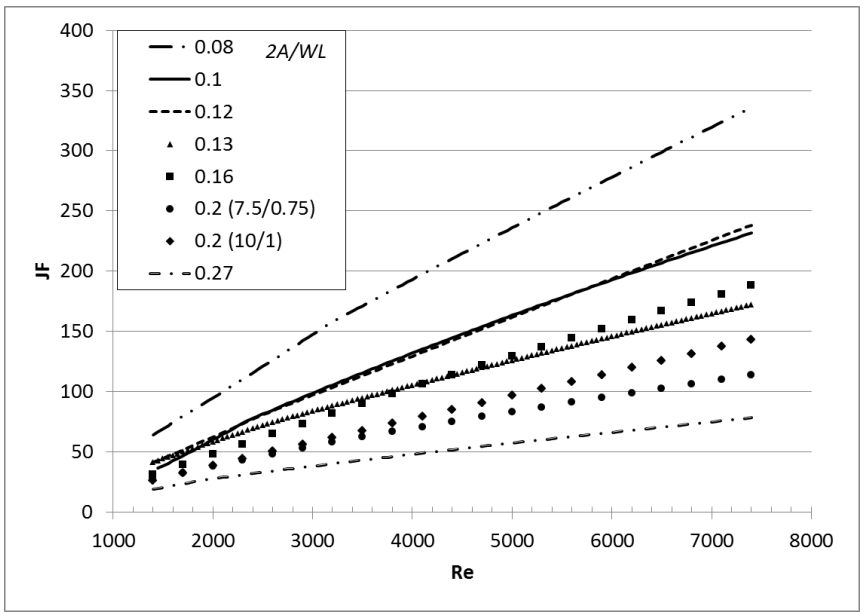

Figure 6. Goodness factor *JF* as function of Reynolds number *Re* for different wavy amplitude wavy length ratios *2A/WL*.

For heat exchanger design quantitative calculations for the thermal hydraulic performance are meaningful, thus figure 7 draw comparision between the experimental data for *Nu* and ψ given and the predicted data given by equations (14-15), derived by multiple regression analysis. Equation 14 can describe 98.7% of *Nu* of the total measurement data within ±20% with an average deviation of 7.7% and equation 15 predicts ψ 52.1% of the total measurement data within ±20% with an average deviation of 25.4%. In comparison to the experimental uncertainties, the experimental correlations do not fit very well to the measurement results, especially for for ψ. This may be due only varying two parameters, the small number of test specimen and the large differences in thermal hydraulic performance. An improved correlation shall be derived by further measurements, i.e. additional geometry parameter variations like fin height, fin pitch, total flow length.

$$Nu = 1.371 * Re^{0.643} * \left(\frac{4F_p}{2A}\right)^{0.435} * \left(\frac{WL}{L}\right)^{-0.212} * \left(\frac{2A}{WL}\right)^{1.108} \quad (14)$$

$$\psi = 2.420 * Re^{-0.223} * \left(\frac{4F_p}{2A}\right)^{-0.272} * \left(\frac{WL}{L}\right)^{-1.603} * \left(\frac{2A}{WL}\right)^{1.149} \quad (15)$$

4. Main conclusions and outlook

A new way of experimental fin development has been proposed in this paper. Test samples were produced by SLM and tested on a thermal hydraulic test bench. A detailed study quantified the impact of geometry parameters wavy length and amplitude on heat transfer and pressured drop. The advantages of SLM for experimental fin development are high dimensional accuracy and degrees of freedom in design, giving opportunity to conduct experimental tests with new fin geometries, not being producable by conventional production techniques. Moreover, as experimental tests are essential

for fin development, the process of fin development can be accelerated by rapid prototyping. The independence of conventional manufacturing processes as another asset gives the chance to conduct geometry parameter variations with state-of-the-art fin geometries, i.e. wavy fins, offset strip fins and louvered fins. Furthermore, simulations and further experiments will be conducted for a more detailed evaluation of the impact of surface roughness.

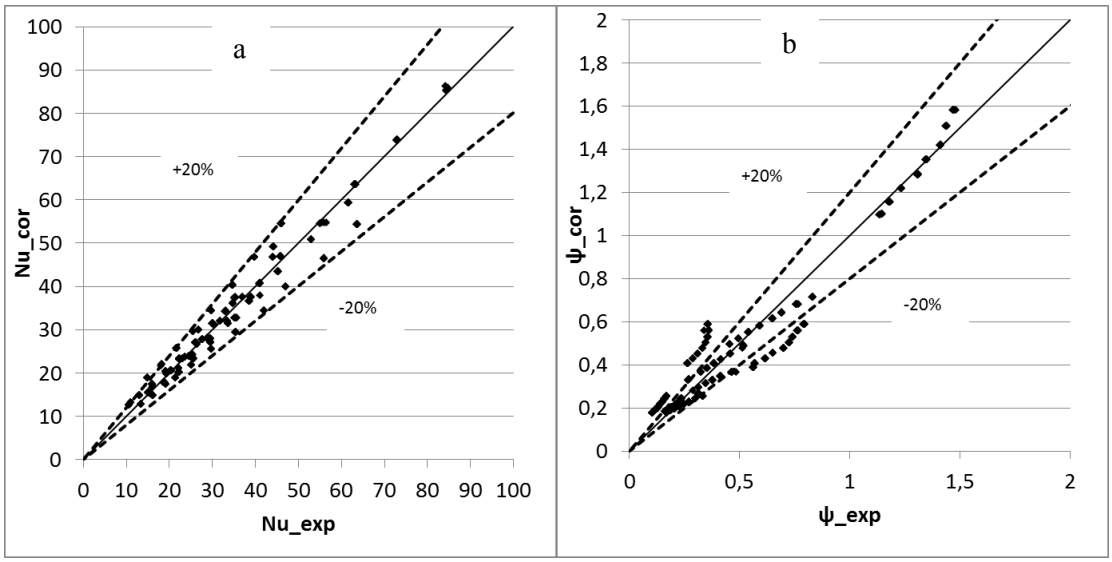

Figure 7. Comparison of experimental data and predicted data for Nusselt number *Nu* (a) and Darcy friction factor ψ (b).

Acknowledgement
The authors acknowledge support from the German Federal Ministry of Economic Affairs and Energy (BMWi) within the frame of "Next Generation Maritime Technologies".

References

[1] Dong J, Su L, Chen Q, and Xu, W 2013 *Appl. Therm. Eng*. **51** 32–39
[2] Comini G, Nonino C and Savino S 2003 *Int. J. Numer. Methods Heat Fluid Flow* **13** 500–519
[3] Dong J, Chen J, Zhang W and Hu J 2010 *Appl. Therm. Eng*. **30** 1377–1386
[4] Dong J, Chen J, Chen Z, Zhou Y and Zhang W 2007 *Applied Thermal Engineering* **27** 306-313
[5] Joshi H M and Webb R L 1987 *Int. J. Heat Mass Transf*. **30** 69–84
[6] VDI Richtlinie 3405 – Blatt 3 2015 *Additive manufacturing processes, rapid manufacturing – Design rules for part production using laser sintering and laser beam melting* (Beuth Verlag: Berlin)
[7] Wong M, Owen I and Sutcliffe C J 2009 *Heat Transfer Engineering* **52** 281-288
[8] Strano G, Hao L, Everson R and Evans K 2013 *Journal of Materials Processing Technology* **213** 589-597
[9] Ventola L, Robotti F, Dialameh M, Calignano F, Manfredi D, Chiavazzo E and Asinari 2014 *Int. J. Heat Mass Transf* **75** 58-74
[10] Schlichting H and Gersten K 2006 *Grenzschicht-Theorie* (Springer-Verlag: Berlin, Heidelberg, New York)
[11] Adams T, Grant C and Watson H 2012 *International Journal of Mechanical engineering and Mechatronics* **2** 66-71